

High Gain Semiconductor Optical Amplifier – Laser Diode at Visible Wavelength

Chao Shen¹, Changmin Lee², Tien Khee Ng¹, Shuji Nakamura², James S. Speck², Steven P. DenBaars², Ahmed Y. Alyamani³, Munir M. El-Desouki³, and Boon S. Ooi^{1*}

¹Photonics Laboratory, King Abdullah University of Science and Technology (KAUST), Thuwal 21534, Saudi Arabia

²Materials Department, University of California Santa Barbara, Santa Barbara (UCSB), CA 93106, United States of America

³King Abdulaziz City for Science and Technology (KACST), Riyadh 11442, Saudi Arabia

* Tel: +966-544700036, Email: boon.ooi@kaust.edu.sa

Abstract—We reported on the first experimental demonstration of a two-section semipolar InGaN-based laser diode with monolithically integrated semiconductor optical amplifier (SOA-LD). The onset of amplification effect was measured at 4V SOA bias (V_{SOA}). The SOA-LD shows a large gain of 5.32 dB at $V_{SOA} = 6$ V.

I. INTRODUCTION

InGaN-based optoelectronic devices, including LEDs, laser diodes (LDs), and waveguide modulators [1-2], have attracted intense research interest for solid-state lighting, visible light communications (VLC), optical storage, display, optical clocking, and sensing applications [3-4]. Yet the semiconductor optical amplifier (SOA) remains a missing component in the violet-blue-green electromagnetic spectrum regime. Integrated SOA is a space- and power- efficient component that enables compact integration and volume manufacturing for high capacity optical communications and high power pulse generation [5-6]. In this work, we demonstrated the first ridge waveguide two-section integrated SOA-LD emitting at ~ 404 nm. The SOA structure is designed to enable electrical isolation and optical coupling with the LD for an effective amplification. The electro-optical properties of the SOA-LD, including an optical gain of 5.32 dB and a gain saturation current of 250 mA were achieved.

II. DESIGN, FABRICATION AND CHARACTERIZATION

Figure 1 presents the device structure of the SOA-LD grown on a semipolar (20 $\bar{2}1$) free-standing GaN substrate using the metal-organic chemical vapor deposition (MOCVD) technique. It consisted of a highly Mg-doped *p*-GaN contact layer, a 600 nm Mg-doped *p*-GaN cladding layer, a 60 nm Mg-doped *p*-InGaN separate confinement heterostructure (SCH) waveguiding layer, a 16 nm Mg-doped *p*-Al_{0.18}Ga_{0.82}N electron blocking layer (EBL), 4-period of 3.6 nm/7 nm In_{0.1}Ga_{0.9}N/GaN multiple quantum-wells (MQWs) active region, a 60 nm Si-doped *n*-In_{0.025}Ga_{0.975}N SCH waveguiding layer, a 350 nm Si-doped *n*-GaN cladding layer, and a highly Si-doped *n*-GaN contact layer. The Pd/Au and Ti/Al/Ni/Au were deposited as *p*- and *n*-GaN metal stacks, respectively.

The fabricated SOA-LD is a three-terminal device consisting of a 300- μ m-long SOA section and a 1190- μ m-long LD section (Fig. 2). The same QW active region layer-

structure was shared by the two sections, which are optically coupled, allowing the emitted light from the LD gain section to be amplified by the integrated SOA section. The 2- μ m-wide ridge waveguide was defined using UV photolithography and plasma etching, and without facet coating. The etching of the isolation trench between the two sections is carefully controlled, providing electrical isolation and maintaining seamless optical coupling. Benefiting from the high lateral resistance of the InGaN waveguiding layer and the AlGaIn EBL, the isolation resistance between the SOA section and LD section is measured to be $\sim M\Omega$, which is more than 5 orders of magnitude higher than the junction series resistance, enabling the independent operation of the two sections.

The device was mounted on thermoelectric cooling (TEC) unit and was tested under continuous wave (CW) operation at room temperature. The laser measurement setup involves a Keithley 2520 DC source and a calibrated Si photodetector incorporated in an integrating sphere for accurate measurement of the optical power *vs.* current (*L-I*) characteristics, a Keithley 2400 source meter for providing SOA driving voltage, an Ando AQ-6315A optical spectrum analyzer for obtaining the emission spectra.

III. RESULTS AND DISCUSSIONS

Figure 3 shows the optical output power of the SOA-LD (*L*) *vs.* driving current in the LD gain region (I_{LD}) characteristics with various voltage biases applied to the waveguide semiconductor optical amplifier (V_{SOA} from 0 V to 6 V). Without any SOA driving voltage ($V_{SOA} = 0$ V), the threshold current (I_{th}) of SOA-LD is 229 mA. Further increase in driving current to $I_{LD} = 250$ mA results in an optical output power of 8.2 mW. With increasing $V_{SOA} > 4$ V applied to the SOA region, increasing optical power and decreasing lasing threshold current are observed in the SOA-LD. The strong V_{SOA} -dependence in optical power is evident in Fig. 4, indicating the amplitude amplification effect. The optical power of SOA-LD at $I_{LD} = 250$ mA is increased to 9.0, 12.9, 17.5, 22.3, and 28.0 mW at $V_{SOA} = 4.0, 4.5, 5.0, 5.5$ and 6.0 V, respectively. The V_{SOA} -associated I_{th} decreasing is presented simultaneously at $V_{SOA} > 4$ V, as shown in Fig. 5. The threshold current of the SOA-LD is reduced to 209, 176, 155, 146, and 138 mA at $V_{SOA} = 4.0, 4.5, 5.0, 5.5$ and 6.0 V, respectively.

The driving voltage applied to the SOA section (V_{SOA}) controls the light output by switching the SOA gain from a low value to a high value. Figure 6 shows the SOA gain curves at an increasing V_{SOA} of 4 V to 6 V in our SOA-LD, which is derived from

$$\text{Gain} = \frac{\text{output power at SOA bias voltage of } V_{SOA}}{\text{output power at zero SOA bias voltage}} \quad (1)$$

The gain saturation is observed at $I_{LD} > 250$ mA. Figure 7 shows the changes of SOA gain at 250 mA as a function of V_{SOA} . The gain increase from 0.41 dB to 5.32 dB, when V_{SOA} increases from 4 V to 6 V, corresponding to a slope of ~ 2.46 dB/V.

To analyze the optical properties of the SOA-LD and support the observation of amplitude amplification effect, we have performed a detailed measurement of the SOA-LD emission spectra at varying I_{LD} and V_{SOA} . Figure 8 features the spectra of the device at $I_{LD} = 160$ mA and increasing V_{SOA} from 0 V to 6 V. The onset of lasing peak at ~ 404 nm is observed at $V_{SOA} > 5$ V with significantly increased peak intensity and narrowed full width at half maximum (FWHM). At $V_{SOA} = 5.5$ V, the FWHM of the emission peak is measured to be 0.68 nm, confirming the appearance of stimulation emission from the SOA-LD. The dependence of the measured FWHM on V_{SOA} at different I_{LD} is summarized in Fig. 9. Based on the narrowing of peak FWHM to < 2 nm, lasing is observed at $V_{SOA} > 5$ V and > 4.5 V for SOA-LD biased at $I_{LD} = 160$ mA and 200 mA, respectively. There is an insignificant change of FWHM and emission wavelength for the lasing peak as the V_{SOA} changes, after the SOA-LD enters stimulated emission regime.

Figure 10 compares the emission spectra of the SOA-LD at $I_{LD} = 200$ mA with $V_{SOA} = 0$ V and 6 V. At $V_{SOA} = 6$ V, The SOA-LD shows a narrow lasing peak at ~ 404 nm. The amplification ratio (R_{amp}), which is derived from the intensity at $V_{SOA} = 6$ V over the intensity at $V_{SOA} = 0$ V, is also plotted as the blue curve. A peak R_{amp} of 16.9 is identified at the lasing wavelength, indicating the effective amplification effect of the integrated SOA. A relative low R_{amp} of ~ 1.5 is measured for the rest of the spectrum range, suggesting a minimized amplification effect for the uncoupled spontaneous component of the emission. For the SOA-LD with a constant driving current in the LD (at $I_{LD} = 200$ mA), the amplification ratio of the emission as a function of the V_{SOA} is plotted in Fig. 11. The increasing of R_{amp} for the lasing peak, from 1.14 to 16.9, is identified with increasing V_{SOA} from 4 V to 6 V, while the R_{amp} remain constant at 1.3 \sim 1.5 for spontaneous emission components. The stimulated emission component is dominantly amplified compared to the spontaneous emission component. Hence, the integrated SOA serves as an efficient amplifier for the demonstrated SOA-LD.

In order to confirm that the measurements and observations of the device performance are solely originating from the amplification effect of the integrated SOA and rule out the possibility that the SOA section works as an independent laser component at high bias (V_{SOA}), we performed the characterization of SOA section without current

injection in the LD section ($I_{LD} = 0$ mA). The relations of optical power vs. current in the SOA section ($L \sim I_{SOA}$) and V_{SOA} vs. I_{SOA} at $I_{LD} = 0$ mA are plotted in Fig. 12 (a) and (b), respectively. At $V_{SOA} = 6$ V, the SOA section has a current of 71 mA, corresponding to a current density of 11.83 kA/cm². From the measured $L \sim I_{SOA}$ relation, we have not observed the onset of stimulated emission or amplified spontaneous emission at I_{SOA} up to 100 mA. This is further supported by the collected emission spectra (as in Fig. 13) from the SOA-LD at $I_{LD} = 0$ mA, as the emission peak shows a large FWHM of > 15 nm at $V_{SOA} = 6$ V, indicating its spontaneous emission nature. Therefore, the observed amplification effect in our presented SOA-LD structure is attributed to the integrated InGaN-based semiconductor optical amplifier.

IV. CONCLUSIONS

In this work, we introduced the integrated short-wavelength semiconductor optical amplifier with laser diode at ~ 404 nm based on InGaN/GaN MQWs. A detailed characterization of the demonstrated SOA-LD reveals the efficient amplification effect in the device, showing a reducing threshold current from 229 mA to 138 mA at $V_{SOA} = 6$ V, and an increasing optical power from 9.0 mW to 28 mW at $I_{LD} = 250$ mA, leading to a large gain of 5.32 dB at $V_{SOA} = 6$ V. Our results clearly demonstrated effective amplification effect achieved using a nitride-based integrated SOA. The SOA-LD, in the violet-blue-green spectrum range, enables high power operation of the laser by extending the thermal roll-over to a significantly higher output power, and is promising for applications in visible-light communications, optical interconnects and photonics integrated circuits.

ACKNOWLEDGMENT

The authors gratefully acknowledge the funding support from King Abdulaziz City for Science and Technology (KACST) Technology Innovation Center (TIC) for Solid State Lighting (KACST TIC R2-FP-008), KACST-KAUST-UCSB Solid-State Lighting Program, and King Abdullah University of Science and Technology (KAUST) (BAS/1/1614-01-01).

REFERENCES

- [1] S. Pimputkar, J. S. Speck, S. P. DenBaars, and S. Nakamura, "Prospects for LED lighting," *Nat. Photon.*, vol. 3, pp. 180-182, Apr 2009.
- [2] C. Shen, T. K. Ng, J. T. Leonard, A. Pourhashemi, H. M. Oubei, M. S. Alias, *et al.*, "High-Modulation-Efficiency, Integrated Waveguide Modulator-Laser Diode at 448 nm," *ACS Photonics*, vol. 3, pp. 262-268, Feb 2016.
- [3] C. Lee, C. Shen, H. M. Oubei, M. Cantore, B. Janjua, T. K. Ng, *et al.*, "2 Gbit/s data transmission from an unfiltered laser-based phosphor-converted white lighting communication system," *Opt. Express*, vol. 23, pp. 29779-29787, Nov 16 2015.
- [4] S. P. DenBaars, D. Feezell, K. Kelchner, S. Pimputkar, C.-C. Pan, C.-C. Yen, *et al.*, "Development of gallium-nitride-based light-emitting diodes (LEDs) and laser diodes for energy-efficient lighting and displays," *Acta Mater.*, vol. 61, pp. 945-951, Feb 2013.
- [5] N. K. Dutta and Q. Wang, *Semiconductor Optical Amplifiers*, World Scientific Publishing Company, 2013.
- [6] K. E. Stubkjaer, "Semiconductor optical amplifier-based all-optical gates for high-speed optical processing," *IEEE J. Sel. Top. Quantum Electron.*, vol. 6, pp. 1428-1435, Nov-Dec 2000.

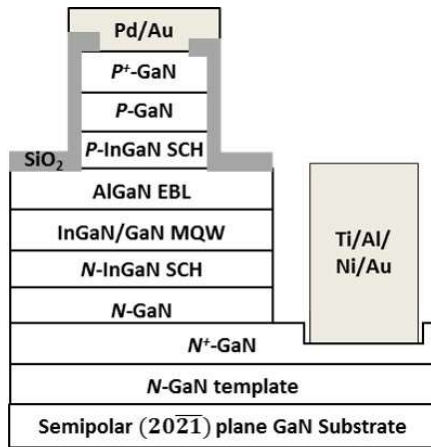


Fig. 1. Cross-section of the device structure.

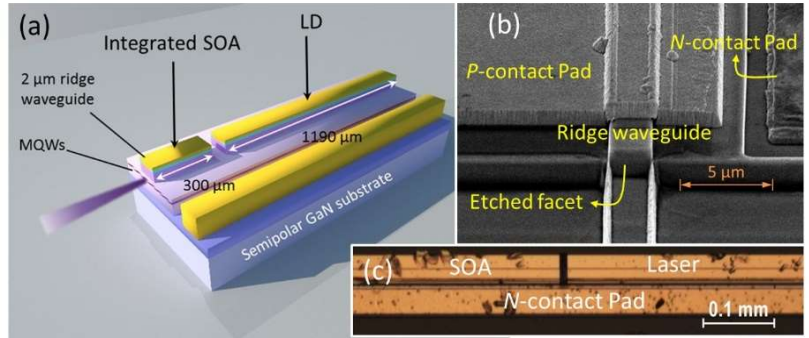


Fig. 2. (a) 3D illustration of the integrated semiconductor optical amplifier-laser diode (SOA-LD), (b) elevation-view scanning electron microscope (SEM) image showing the facet of the SOA-LD and (c) top-view optical microscope image of the SOA-LD. The scale bars for (b) and (c) are 5 μm and 100 μm , respectively.

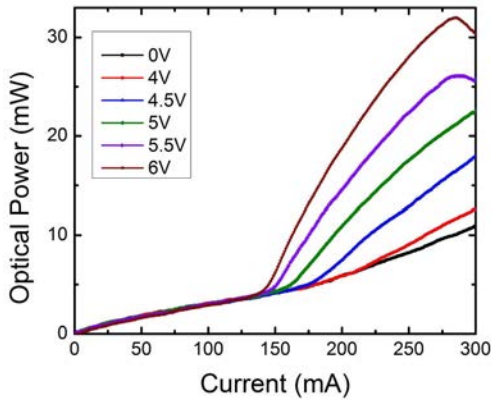


Fig. 3. Light output power vs. driving current in the LD region (I_{LD}) relations of SOA-LD with varying bias voltage in SOA section (V_{SOA}).

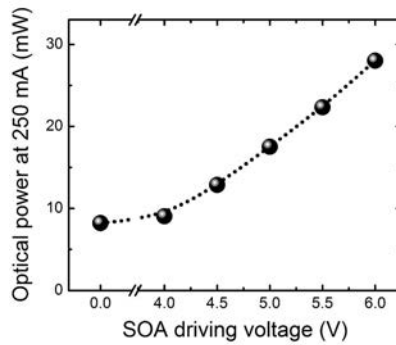


Fig. 4. Plot of optical power at $I_{LD} = 250$ mA vs. SOA driving voltage (V_{SOA}).

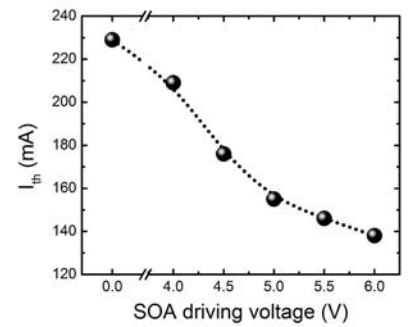


Fig. 5. Plot of threshold current of the SOA-LD (I_{th}) vs. V_{SOA} .

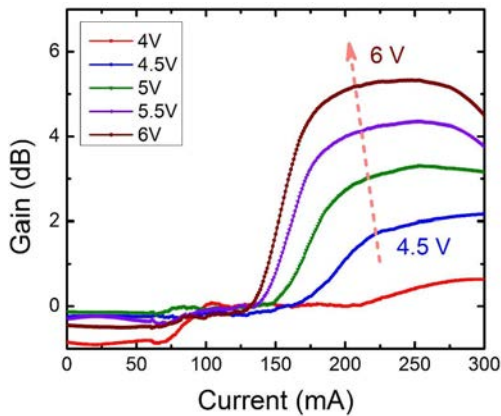


Fig. 6. Gain vs. I_{LD} relation of the SOA-LD. The gain is calculated from the ratio of output optical power at SOA bias voltage of V_{SOA} over output optical power at zero SOA bias.

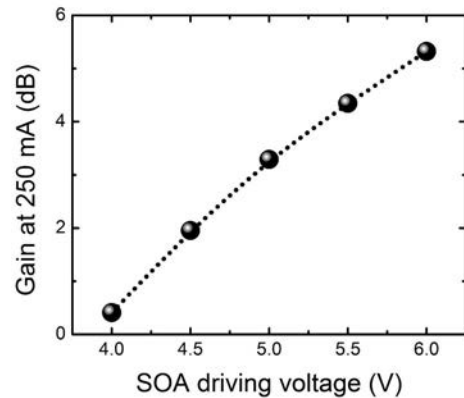


Fig. 7 Measured SOA gain at $I_{LD} = 250$ mA as a function of V_{SOA} .

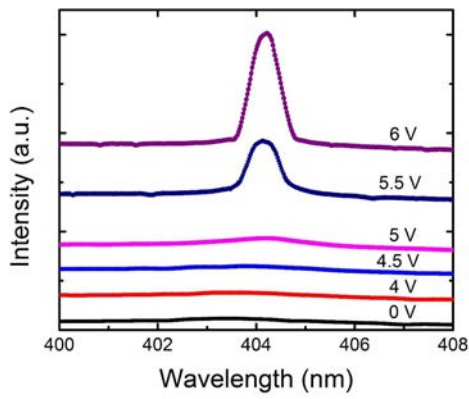


Fig. 8. Emission spectra of the SOA-LD at $I_{LD} = 160$ mA with different V_{SOA} .

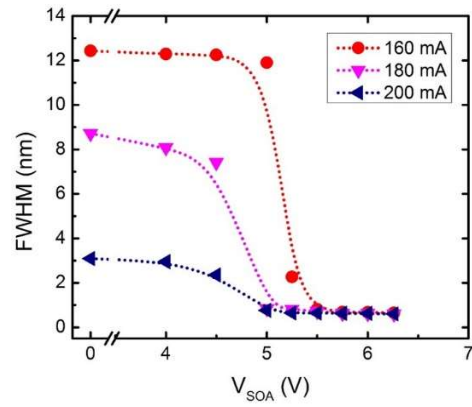


Fig. 9. Plot of full width at half maximum (FWHM) of the SOA-LD emission spectra vs. V_{SOA} at I_{LD} of 160 mA ~ 200 mA.

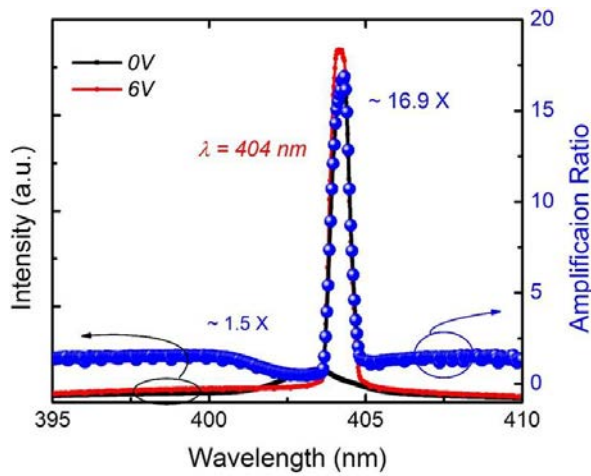


Fig. 10. Emission spectra of SOA-LD at $I_{LD} = 200$ mA with $V_{SOA} = 0$ V and 6V, respectively. The amplification ratio vs. wavelength is plotted. The amplification ratio (R_{amp}) is defined as the intensity at $V_{SOA} = 6$ V over the intensity at $V_{SOA} = 0$ V.

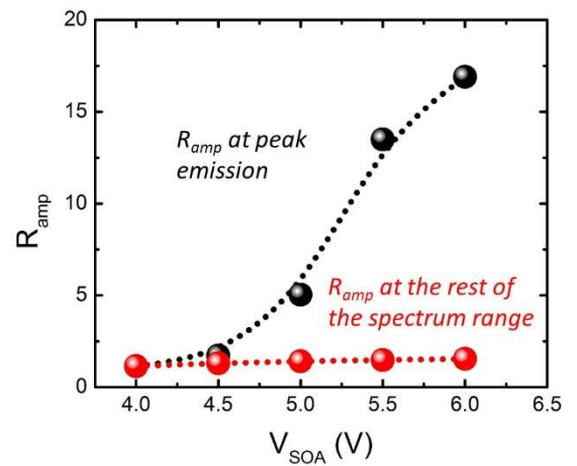


Fig. 11 Amplification ratio of the SOA-LD as a function of V_{SOA} . The black symbols represent the R_{amp} at the peak emission, i.e. the stimulated emission component, while the red symbols are the R_{amp} at the rest of the spectrum range, i.e. the spontaneous emission component.

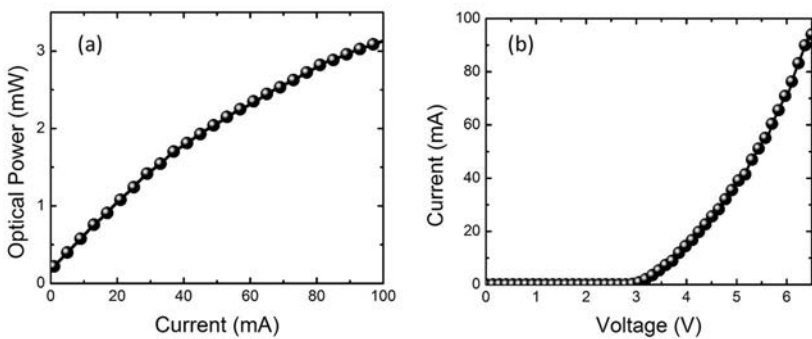


Fig. 12. Plots of (a) optical power vs. current in the SOA section (I_{SOA}) and (b) I_{SOA} vs. V_{SOA} at $I_{LD} = 0$ mA.

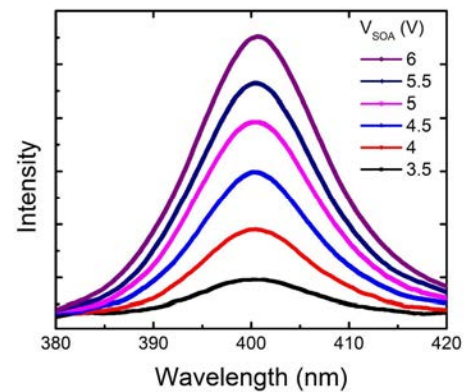


Fig. 13 Emission spectra of the SOA section at $I_{LD} = 0$ mA with different V_{SOA} .